

## Ionization of Helium in the Attosecond Equivalent Light Pulse of 1 GeV/Nucleon $U^{92+}$ Projectiles

R. Moshhammer,<sup>1</sup> W. Schmitt,<sup>2</sup> J. Ullrich,<sup>2</sup> H. Kollmus,<sup>1</sup> A. Cassimi,<sup>3</sup> R. Dörner,<sup>1</sup> O. Jagutzki,<sup>1</sup>

R. Mann,<sup>2</sup> R. E. Olson,<sup>4</sup> H. T. Prinz,<sup>2</sup> H. Schmidt-Böcking,<sup>1</sup> and L. Spielberger<sup>1</sup>

<sup>1</sup>*Institut für Kernphysik, Universität Frankfurt, D-60486 Frankfurt am Main, Germany*

<sup>2</sup>*Gesellschaft für Schwerionenforschung, D-64291 Darmstadt, Germany*

<sup>3</sup>*Centre Interdisciplinaire de Recherches avec les Ions Lourds, F-14040 Caen Cedex, France*

<sup>4</sup>*Department of Physics, University of Missouri—Rolla, Rolla, Missouri 65401*

(Received 14 July 1997)

Single and double ionization of helium by 1 GeV/nucleon  $U^{92+}$  impact was explored in a kinematically complete experiment. The relativistic ion generates a subattosecond ( $10^{-18}$  s) superintense ( $I > 10^{19}$  W/cm<sup>2</sup>) electromagnetic pulse, which is interpreted as a field of equivalent photons (Weizsäcker-Williams method). Cross sections, the emission characteristics of ions and electrons as well as momentum balances, are quantitatively discussed in terms of photoionization of the atom in this broadband, ultrashort virtual photon field. [S0031-9007(97)04437-2]

PACS numbers: 34.10.+x, 34.50.Fa

The dynamical behavior of atoms, molecules, clusters, or solids exposed to strong electromagnetic fields has become a subject of enormous recent attention fueled by the rapid development of superintense femtosecond lasers [1] and possible applications. Among many other results it has been demonstrated that atoms can be multiply ionized in such pulses (see, e.g., [2,3]). In parallel, for more than a decade it has been known that relativistic highly charged ions can cause up to 30-fold ionization of heavy target atoms in one single collision with cross sections close to  $10^{-17}$  cm<sup>2</sup> (see, e.g., [4,5]). The fields generated by these ions at the target atom exceed power densities of  $10^{19}$  W/cm<sup>2</sup>, and pulse times are typically well below attoseconds. For both situations, mainly total cross sections or ion yields have been reported. Details about the dynamics of these exotic ionization processes essentially remained unexplored up to now.

The fact that the interaction of energetic charged particles and photons with matter are of common nature was recognized very early by Fermi, Weizsäcker, and Williams [6] and has been widely used since then, mainly in nuclear physics (see, e.g., [7]). In this approach, the time and impact-parameter dependent electromagnetic field of the passing projectile  $[E(t, b)]$  is decomposed into two pulses propagating along and transverse to the projectile velocity. Fourier transformation  $[E(\omega, b)]$  and subsequent quantization yield two pulses of equivalent photons carrying a number of  $n(\omega, b)$  photons incident on the atom per unit area and frequency interval  $d\omega$ . Ionization of a target atom is simply described as “photoionization” by this field of equivalent photons of various frequencies. Depending on its intensity, i.e., on the charge state  $q$  and on the velocity  $v_P$  of the generating projectile, one or several virtual photons might be absorbed or scattered within the pulse leading to single or multiple target ionization.

Several recent theoretical publications have been devoted to come to a detailed understanding of this equivalent

lence [8–11]. Charged particle induced dipole transitions at a specific energy loss  $\Delta E_P$  of the projectile have been related to the absorption of a photon with an energy of  $E_\gamma = \Delta E_P$ . The nondipole transitions which are always present for charged particle impact have been related to Compton scattering occurring at high photon energies [10]. The simultaneous absorption of two photons during one collision has been investigated recently [11] to explore the role of the initial state electron-electron correlation in comparison with first kinematically complete experiments on double ionization of helium by nonrelativistic highly charged particle impact [12].

In contrast, no differential experiments have been reported until now investigating the target ionization dynamics in the superintense and ultrashort electromagnetic pulses generated by relativistic highly charged ions and its equivalence to photoionization. Pulse times are 4 orders of magnitude shorter than obtainable by the most advanced high-power femtosecond lasers and intensities are orders of magnitude larger than those provided by any modern synchrotron radiation facility.

In this Letter we report on the first kinematically complete experiment on single and double ionization of helium by relativistic highly charged ion impact. Exploiting coincident multielectron recoil-ion momentum spectroscopy the complete momentum vectors of all emerging target fragments have been measured for 1 GeV/nucleon  $U^{92+}$  on helium collisions. The energy loss of the projectile  $\Delta E_P$  has been determined from energy conservation for each single encounter with a resolution of 0.1 to 15 eV (for  $0 < \Delta E_P < 150$  eV), corresponding to an unprecedented accuracy for the relative energy loss of  $4 \times 10^{-13} < \Delta E_P/E_P < 6 \times 10^{-11}$ . This enabled a precise comparison of differential ionization cross sections for fast particle impact with differential photoionization cross sections at well defined  $\Delta E_P = E_\gamma$  and provided first insight into the dynamic response of an atom exposed to electromagnetic

fields that are stronger and shorter than ever investigated before.

The experiments were performed at the heavy-ion synchrotron SIS of GSI (Gesellschaft für Schwerionenforschung) using a well focused (2 mm × 2 mm) 1 GeV/nucleon bare uranium beam. Typical intensities ranged up to  $10^7$  particles per spill at a spill length of 8 s counted by a fast scintillation detector. A two-stage supersonic jet provided a well defined (2.8 mm diameter), cold (50 mK), and dense ( $10^{12}$  atoms per  $\text{cm}^2$ ) helium target. Low-energy ions (typical energies  $E_R < 50$  meV) and electrons (typical energies  $E_e < 80$  eV) are accelerated into opposite directions by applying a weak electric field (1–5 V/cm) along the ion beam. The field is sufficiently strong to project recoiling target ions with a large solid angle ( $\Delta\Omega_R/4\pi > 98\%$  for  $\text{He}^{1+,2+}$ ) onto a two-dimensional position sensitive microchannel plate detector (MCP). An additional solenoidal magnetic field is generated by two Helmholtz coils (1.5 m diameter) with its field vector along the ion beam. It efficiently guides the electrons ( $\Delta\Omega_e/4\pi > 50\%$ ) onto a 80 mm diameter MCP equipped with a fast delay-line readout that is capable of accepting “multihits” for time intervals between individual hits larger than 10 ns. From the measured absolute positions and flight times the ion and electron trajectories are reconstructed and their initial momenta are calculated. (For details of the “GSI reaction microscope” see [12,13]; for a recent review on the field see [14].) Absolute cross sections are obtained by integration over all final momentum components and normalization to previously measured values of  $7.4 \times 10^{-16}$   $\text{cm}^2$  for single and  $1.5 \times 10^{-17}$   $\text{cm}^2$  for double ionization [19] which are accurate within  $\pm 30\%$ .

The equivalent photon approximation (EPA) to describe relativistic collisions has been discussed in detail in numerous publications (see, e.g., [7,11]). The basic idea is to describe the Lorentz transformed Coulomb field of the projectile [charge  $q$ , impact parameter  $b$ , Lorentz factor  $\gamma = 1/\sqrt{1 - (v_P/c)^2}$ ] at the target in terms of two pulses of linear polarized virtual photons with frequency  $\omega$  propagating along ( $\parallel$ ) and transverse ( $\perp$ ) to the straight line projectile trajectory ( $c$  is the velocity of light,  $K_{0,1}$  are modified Bessel functions; atomic units are used throughout):

$$n_{\parallel}(b, \omega) = (q/\pi)^2 c^{-1} (\omega c / \gamma v_P^2)^2 K_1^2(\omega b / \gamma v_P), \quad (1)$$

$$n_{\perp}(b, \omega) = (q/\pi)^2 c^{-1} (\omega c / \gamma v_P^2)^2 (1/\gamma^2) K_0^2(\omega b / \gamma v_P). \quad (2)$$

Differential ionization cross sections  $d\sigma(b, \chi_f)$  can now be calculated in terms of the equivalent photon induced cross sections  $d\sigma_{\gamma}(\omega, \chi_f)$  where  $\chi_f$  denotes the set of final state quantum numbers,

$$d\sigma(b, \chi_f) = \sum \int (1/\omega) n(b, \omega) d\sigma_{\gamma}(\omega, \chi_f) d\omega. \quad (3)$$

The applicability of the method is restricted to distant collisions and is inappropriate if the projectile penetrates

the target system. It thus requires the introduction of a lower cutoff impact parameter  $b_{\min}$  (see, e.g., [7,11] and references therein) which should be larger than the spatial extension of the He wave function and was chosen to be 1 a.u. in the present calculations. Furthermore, contributions of the various frequencies are added incoherently, which is only reasonable if the projectile can be considered to be a small perturbation.

In Fig. 1 the final state momentum distributions projected onto the collision plane are shown for both the electron  $\mathbf{p}_e$  and the recoiling  $\text{He}^+$  target ion  $\mathbf{p}_R$  after single ionization of He. The collision plane is defined by the incoming projectile momentum vector propagating along the positive  $p_{\parallel}$  axis and the vector of the recoiling target ion along the negative  $p_x$  direction (bold letters denote two-dimensional vectors in this plane). The following features are observed:

First, for each singly ionizing collision the emitted electron and the recoiling  $\text{He}^+$  ion emerge into opposite directions with  $\mathbf{p}_R \approx -\mathbf{p}_e$ . The event-by-event analysis shows that their momenta compensate on the level of the experimental resolution of  $\sqrt{\Delta p_e^2 + \Delta p_R^2} = 0.3$  a.u. Thus, the momentum change of the projectile  $\Delta \mathbf{p}_P = -(\mathbf{p}_R + \mathbf{p}_e)$  is very small. Such a result is not trivial in the transverse direction but follows from momentum conservation along the longitudinal axis: For small energy losses of the projectile, i.e., for continuum electron energies  $E_e < 100$  eV, one obtains  $\Delta p_{P\parallel} = \Delta E_P / v_P < 0.03$  a.u. For the present projectile velocity of  $v_P = 0.88c$  this exceeds the momentum transfer for photoabsorption  $p_{\gamma} = E_{\gamma}/c$  leading to the same final state electron energy  $E_e = E_{\gamma} - E_{\text{bind}}$  by only about 12% ( $E_{\text{bind}}$ : He ionization potential).

Second, the distributions are centered around  $p_{\parallel} = 0$ . At lower projectile energies a forward-backward asymmetry had been observed before [12,15,16] which was interpreted as a post collision interaction (PCI) of the emerging highly charged projectile with the target fragments pulling

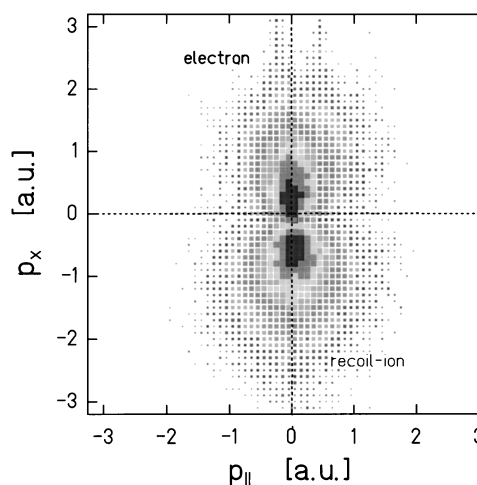


FIG. 1. Momentum distribution of the electron and the recoiling target ion projected onto the collision plane (see text) for 1 GeV/nucleon  $\text{U}^{92+}$  on He singly ionizing collisions.

the electron behind and pushing the recoil ion away. In the present case the PCI becomes negligibly small, and the final momenta of the electron and the recoil ion are essentially unaffected by the rapidly emerging uranium ion. This is an effect of both the smaller perturbation and the relativistic contraction of the Coulomb field in the target frame along the projectile propagation [17]. Thus, the complicated final state three-particle continuum has effectively collapsed to a two-particle continuum as in photoionization where the photon is absorbed and not present in the final state.

Third, the distributions mainly extend into the transverse direction. This is due to the fact that the longitudinal component of the force, which is relativistically reduced by  $1/\gamma^2$  [17], averages to zero when integrated over the whole collision time.

In summary, the atoms seem to “explode” in the field of the projectile delivering energy but “no” momentum. Surprisingly, the fast highly charged projectile carrying 0.24 TeV kinetic energy does not destroy the target in a severe collision with high momentum transfers but rather acts in a very gentle way for the majority of the collision events. Since the observed final momenta of the electron and of the recoil ion were not transferred by the projectile during the collision, they must have been stored in the atom before and therefore reflect the Compton profile of the initially bound electron.

All these features are consistent with the characteristics of ionization by linear polarized (along the  $p_x$  axis) photons of different incident energies. Performing a simple calculation within the EPA using experimental cross sections  $d\sigma_\gamma(\omega, \chi_f)$  for single photoionization of helium [18] this has been investigated quantitatively. The results are shown in Fig. 2 where the two-dimensional momentum distributions of Fig. 1 have been projected onto the longitudinal axis for a better comparison. The calculated

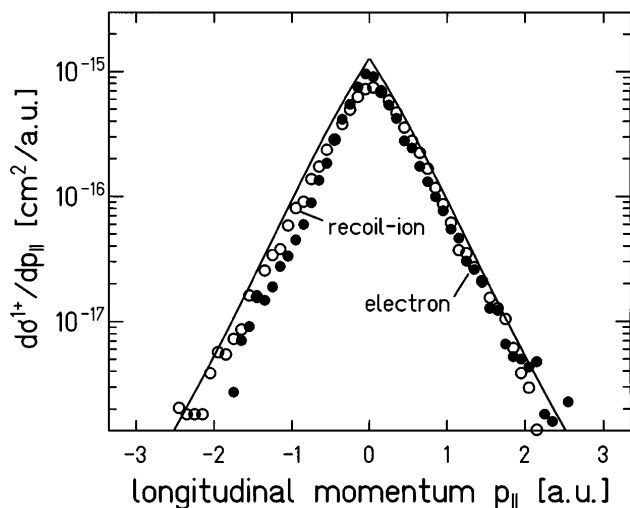


FIG. 2. Longitudinal momentum distribution of the recoil ion (open circles) and the electron (solid circles) for 1 GeV/nucleon  $U^{92+}$  on He single ionization. Full curve: Theory (see text).

electron and recoil-ion momenta are identical on the level of the incoming photon momentum which is less than 0.03 a.u. (for  $E_e < 100$  eV). Excellent agreement with the experimental data is obtained in the shape of the distribution as well as in the absolute magnitude of the cross section. The  $p_{\parallel}$  dependence was found to be very insensitive to the *ad hoc* choice of the lower impact parameter  $b_{\min}$ . In essence, it mainly depends on the photoionization cross section which is sensitive to the bound state He wave function. In contrast, the total cross section varies by about 30% for a reasonable choice of  $1 < b_{\min} < 3$  a.u. One should keep in mind that this is within the experimental uncertainty in the total cross section measurement [19].

Knowing the number of virtual quanta per unit energy interval in the charged particle induced field, the photoionization cross section as a function of  $E_\gamma$  can be obtained from the measured cross section for defined energy loss of the projectile  $\Delta E_P = E_\gamma = E_e + E_{\text{bind}}$ . This is demonstrated in Fig. 3 where the present results are compared with recommended values for  $\sigma_\gamma(\omega)$  of helium obtained using single photons from synchrotron radiation sources [18].

The excellent description of experimental data within the EPA is surprising for several reasons: First, the perturbation strength of the 1 GeV/nucleon  $U^{92+}$  projectile  $q/v_P = 0.76$  cannot be considered to be small, but is close to unity. Second, the applicability of the model has been estimated to be limited to energies larger than “at least a few GeV/nucleon” [11]. Third, spin-flip contributions and magnetic transitions are not incorporated but might become important.

Finally, cross sections differential in the energy of one emitted electron  $d\sigma/dE_e$  for single and double ionization are displayed in Fig. 4, and low-energy electrons are

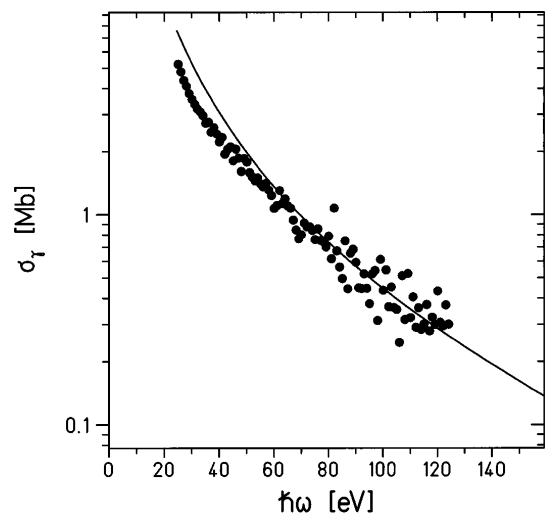


FIG. 3. Absolute cross section for single photoionization of He as a function of the photon energy. Solid circles: Present results for equivalent photons with energies  $\hbar\omega = \Delta E_P$  (see text). Full line: Recommended values from measurements using single monochromatic photons from synchrotron radiation facilities.

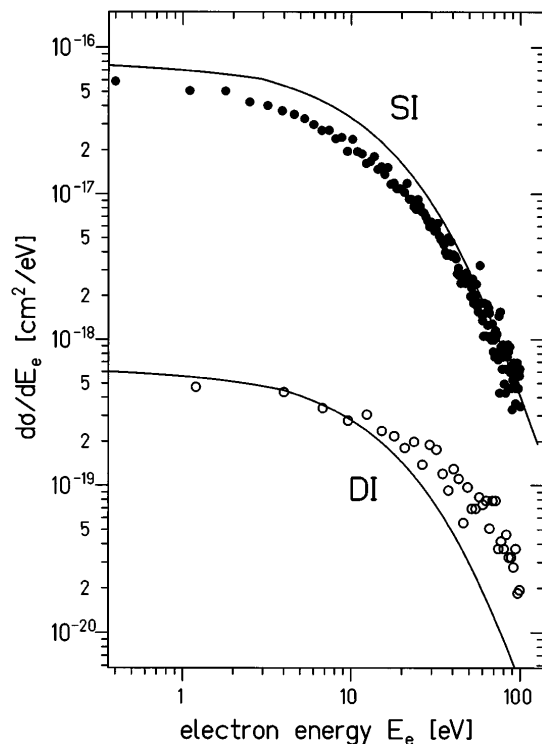


FIG. 4. Single differential cross sections  $d\sigma/dE_e$  for electron emission in 1 GeV/nucleon  $U^{92+}$  on He collisions. Solid circles: Experimental data for single ionization (SI). Open circles: Experimental data for double ionization (DI). Lines: Calculations (see text).

observed to strongly dominate the spectrum for both reactions. Thus, dipole transitions related to low-energy transfers by the projectile close to the single or double ionization thresholds are found to be most important. For a simple estimate of the double ionization differential cross section  $d\sigma/dE_e$  within the EPA it was assumed that two virtual photons are absorbed during one collision. That is, both electrons are emitted as a result of independent interactions with the projectile. From numerous total cross section measurements and theoretical calculations it has become commonly accepted that such a “two-step” mechanism predominantly contributes to double ionization for perturbations by the projectile of  $q/v_P > 0.2$  [5]. Whereas the two photon density  $n(\omega_1, \omega_2)$  is well defined, a choice had to be made concerning the photoionization cross section for each of the electrons (this ambiguity is inherent to any independent particle calculation). The radial electron-electron correlation was partly considered by using an independent event model taking the correct photoionization cross section of atomic He for the first electron and a hydrogenlike  $He^+(1s)$  wave function to calculate the absorption cross section for the second one. The energy distribution of the first electron has been obtained by integrating over the second electron and vice versa. These two single differential cross sections have been averaged to approximate a typical electron emitted in a doubly ionizing collision. Surprisingly, such a simple calculation does fairly well predict

the total as well as the single differential electron emission cross section as a function of the energy of one emerging electron.

In summary, we have performed the first kinematically complete experiment on single and double ionization of helium by relativistic highly charged ion impact exploring the collision dynamics in unprecedented detail. Within the Weizsäcker-Williams equivalent photon method the 1 GeV/nucleon  $U^{92+}$  projectile has been interpreted as a source of an attosecond, exawatt/cm<sup>2</sup>, broadband virtual photon pulse that cannot be provided by any other source of radiation. The fundamental relationship between ionization by charged particles and photons was investigated, and calculations in the EPA were found to be in excellent agreement with the experimental data for single ionization. Double ionization was well described assuming the exchange of two virtual photons as the predominant mechanism. Future kinematically complete experiments will be devoted to explore and compare the role of the electron-electron correlation for double ionization of helium in the attosecond electromagnetic fields of highly charged fast projectiles and in femtosecond intense laser fields. The latter seem to be feasible after some modifications of our apparatus and are presently under preparation.

We would like to thank the SIS crew of GSI for providing an excellent beam and are grateful to S. Keller, H. J. Lüdde, and R. Dreizler for numerous discussions. This work was supported by Gesellschaft für Schwerionenforschung, Bundesministerium für Bildung und Forschung, Deutsche Forschungsgemeinschaft, and the National Science Foundation Int-9112815.

- 
- [1] M. D. Perry and G. Mourou, *Science* **264**, 917 (1994).
  - [2] A. L’Huillier *et al.*, *Phys. Rev. A* **27**, 2503 (1983).
  - [3] J. B. Watson *et al.*, *Phys. Rev. Lett.* **78**, 1884 (1997).
  - [4] S. Kelbch *et al.*, *J. Phys. B* **17**, L785 (1984).
  - [5] J. Ullrich *et al.*, *Phys. Rev. Lett.* **71**, 1697 (1993).
  - [6] C. F. Weizsäcker, *Z. Phys.* **88**, 612 (1934); E. J. Williams, *Phys. Rev.* **45**, 729 (1934).
  - [7] C. Bertulani and G. Baur, *Phys. Rep.* **163**, 299 (1988).
  - [8] J. Wang, J. H. McGuire, and J. Burgdörfer, *Phys. Rev. A* **51**, 4687 (1995).
  - [9] S. T. Mason and J. H. McGuire, *Phys. Rev. A* **51**, 400 (1995).
  - [10] J. Wang *et al.*, *Phys. Rev. Lett.* **77**, 1723 (1996).
  - [11] S. Keller, H. J. Lüdde, and R. M. Dreizler, *Phys. Rev. A* **55**, 4215 (1997).
  - [12] R. Moshhammer *et al.*, *Phys. Rev. Lett.* **77**, 1242 (1996).
  - [13] R. Moshhammer *et al.*, *Nucl. Instrum. Methods Phys. Res., Sect. B* **108**, 425 (1996).
  - [14] J. Ullrich *et al.*, *J. Phys. B* **30**, 2917 (1997).
  - [15] R. Moshhammer *et al.*, *Phys. Rev. Lett.* **73**, 3371 (1994).
  - [16] R. Moshhammer *et al.*, *Phys. Rev. A* **56**, 1351 (1997).
  - [17] Ch. Wood *et al.* (to be published).
  - [18] G. V. Marr and J. B. West, *At. Data Nucl. Data Tables* **18**, 497 (1976).
  - [19] H. Berg *et al.*, *J. Phys. B* **25**, 3655 (1992).